Site selection for Extremely Large Telescopes using the FriOWL software and global re-analysis climate data

E. Graham (1), M. Sarazin (2), H, Kurlandczyk (2), M. Neun (3), C. Mätzler (1)

(1) Institute of Applied Physics, Sidlerstrasse 5, University of Bern, CH-3012, Switzerland
(2) European Southern Observatory, Karl-Schwarzschildstrasse 2, Garching bei Münichen, D-85748, Germany
(3) Department of Geography, Winterthurerstrasse 190, University of Zurich, CH-8057, Switzerland

ABSTRACT

FriOWL is a site selection tool for large or extremely large telescope projects. It consists of a graphical user interface and a large global climatic and geophysical database, and is directly accessible on the world wide web. A new version (version 3.1) of the software has recently been developed by scientists at the University of Bern (Switzerland) and European Southern Observatory (Germany).

The main feature of the new FriOWL database is the inclusion of ERA40 re-analysis data, giving access to over 40 years of long-term climate data. New software tools, programmed in the style of a Geographical Information System, include the capability of resampling layers and time series extraction. A new global seismic hazard layer has been introduced, as well as very high resolution (1km) topographic tiles. Reclassification and overlaying of layers is also possible.

Although FriOWL is primarily designed for site selection projects, it can equally be used in other climate studies. It is especially important in the determination of the climatic stability of a potential site, and in the analysis of climatic anomalies and trends. The long-term astroclimatological seeing and photometric statistics for the Paranal and La Silla observatories can be used to validate FriOWL. A case study of ESO Paranal using FriOWL reveals that the deterioration in seeing conditions since 1998 is related to a strong increase in 1000 hPa geopotential height to the south-east of the observatory; there may also be a link with the Interdecadal Pacific Oscillation.

Keywords: Astroclimatology, FriOWL, Extremely Large Telescopes, site selection, climate change, re-analysis, re-analyses, seeing, E-ELT, Paranal

1. INTRODUCTION

The "FriOWL" project started in 2002 as a joint project between the European Southern Observatory (ESO) and the University of Fribourg, Switzerland. The project goal was to help find the best site(s) in the world for the 100-metre wide OverWhelmingly Large (OWL) telescope, by using a combination of long series of global climatic information (known as "re-analyses") and a Geographical Information System (GIS) as a site selection tool. Thus the original "*FriOWL*" acronym was born (from a combination the names "Fribourg" and "OWL") .

Late in 2006, however, OWL was dropped by ESO in favour of the more modest (yet still very large) 40-metre wide European Extremely Large Telescope (E-ELT). At around the same time, the *FriOWL* project base in Switzerland moved from the University of Fribourg to the nearby University of Bern, Despite these changes, the *FriOWL* name endured and has continued in use since then, and has now grown to encompass many different aspects of site selection for telescopes, as well as having other new climatological uses[1]. Nevertheless, it is proposed to replace the *FriOWL* acronym soon with a new name which appropriately reflects the arrival of new E-ELT era (see section 6).

The main objective of the *FriOWL* project has been to gather together all of the global geophysical parameters that influence site selection for large telescopes into a single database, to make this database easily accessible under one single web portal or computing interface, and for the interface itself to be able to act as a tool in the search for, and classification of, worldwide candidate sites or regions.

2. DESCRIPTION OF THE FRIOWL TOOL AND DATABASE

The *FriOWL* tool consists of a Graphical User Interface (GUI) computer application, directly accessible on the World Wide Web[†], and a large database of long-term global geophysical information (climatological and geomorphological data). The GUI has been designed specifically to interact with the database in a quick and user-friendly fashion through the use of GIS-like interrogation and manipulation functions. A GIS (Geographical Information System) is a computer software which can analyse spatial information of a geographical nature, allowing tasks such as overlaying, reclassifying or resampling of data layers. Importances or weightings may then be given to some layers to give precedence over others. For further information on the design, structure and operation of *FriOWL*, please see [1, 2, 3].

2.1 Access to *FriOWL* and new software improvements

FriOWL is written in the Java computing language; the only pre-requisite for use is that the user has the Java Runtime Environment installed on their internet browser (minimum version required at the time of writing is Java 1.5). A username and password are also necessary to operate the software - these can be requested by filling out the '*Contact us*' form on the FriOWL website[‡], or by emailing the authors of this manuscript. The most recent version of *FriOWL* is version 3.1 (from now on referred to as '*FriOWL-v3.1*') and represents a significant improvement over previous *FriOWL* version 2.1[4]. New software tools, such as the capability to resample, reclassify and overlay layers of different resolution have been introduced. A new time series extraction feature has been added. The user can now also save or download data in a variety of image and text formats.

2.2 The new *FriOWL-v3.1* database

Of particular interest in the new database are the new long-term (> 40 years) global climatological datasets known as 're-analyses', especially ERA40. Re-analyses are reconstructions of past weather conditions using the state-of-the-art data assimilation and numerical weather prediction models of today[2, 5, 6]. Thus, the accuracy of the re-analyses are not constrained by improvements or changes in weather forecasting accuracy over the past 40 years, but are limited only by the availability of observations and the physics of the numerical model itself. ERA40 is generally regarded as the most accurate re-analysis to date[6].

The full *FriOWL-v3.1* database is listed in Table 1. Of particular note are the availability of ERA40 cloud cover, partially integrated water vapour, windspeed, geopotential and vertical velocities datasets at various vertical levels. A new global seismic risk layer at high resolution has also been introduced[7], as well as extremely high resolution (1km) topographic tiles from the United States Geological Survey[8]. Cloud cover data for the future (2021-2030) from the Canadian General Circulation Model has also been introduced as a special test[9]. For a detailed examination and discussion of the re-analyses datasets, and many more results relating to the *FriOWL* project, please see [1] and associated documents (available online[†‡]).

Table 1 (overleaf): The complete *FriOWL-v3.1* database, listed according to source (model or origin of dataset), meteorological or geophysical parameter, vertical atmospheric levels for which the parameter is provided, SI units of the parameter, horizontal resolution (degrees latitude / longitude), time resolution and period of availability.

† *http://archive.eso.org/friowl-45/*
‡ *http://archive.eso.org/friowl-45/friowl_contact_us.php*
†‡ *http://www.iapmw.unibe.ch/research/projects/FriOWL/friowl_users_guide.php*

Source	Parameter	Levels	Units	Resolution (Lat / Lon)	Time Resolution	Period Available
ERA-40	Air temperature	surface	K	2.5° X 2.5°	monthly means of 00, 06, 12, 18 UTC	9/1957 to 8/2002
	Dewpoint	surface	K	2.5° X 2.5°	monthly means of 00, 06, 12, 18 UTC	9/1957 to 8/2002
	Cloud cover	high medium low total	0 to 1	2.5° X 2.5°	monthly means of 00, 06, 12, 18 UTC	9/1957 to 8/2002
	Integrated water vapour (IWV)	500 hPa 600 hPa 700 hPa 800 hPa	kg/m² (mm)	2.5° X 2.5°	monthly means	9/1957 to 8/2002
	Windspeed	200 hPa 500 hPa 700 hPa 1000 hPa	m/s	2.5° X 2.5°	monthly means	9/1957 to 8/2002
	Geopotential height	200 hPa 500 hPa 700 hPa 1000 hPa	dam	2.5° X 2.5°	monthly means	9/1957 to 8/2002
	Vertical velocities	200 hPa 250 hPa 300 hPa 400 hPa 500 hPa 600 hPa 700 hPa 775 hPa	m/s	2.5° X 2.5°	monthly means	1/1991 to 12/2000
	Orography / topography	surface	m	2.5° X 2.5°	time-invariant fields	
	Standard deviation of orography	surface	m	2.5° X 2.5°		
	Land-sea mask	surface	0 or 1	2.5° X 2.5°		
	Low vegetation	surface	0 to 1	2.5° X 2.5°		
	High vegetation	surface	0 to 1	2.5° X 2.5°		
NCEP-NCAR	Air temperature	surface	°C	2.5° X 2.5°	monthly means	1/1948 to 8/2007
	Geopotential height	200 hPa 500 hPa 700 hPa 1000 hPa	dam	2.5° X 2.5°	monthly means	1/1948 to 9/2007
	Total column precipitable water (PR_WTR; same as IWV)	surface	kg/m² (mm)	2.5° X 2.5°	monthly means	1/1948 to 6/2007
	Orography	surface	m	2.5° X 2.5°	time-invariant field	
NOAA	Outgoing longwave radiation (OLR)	top of atmosphere	W/m²	2.5° X 2.5°	monthly means	6/1974 to 3/2007
CGCM1	Cloud cover	total cover	0 to 1	3.75° X 3.75°	monthly means	1/1991 to 12/2000 (simulation)
	Cloud cover	total cover	0 to 1	3.75° X 3.75°	monthly means	1/2021 to 12/2030 (simulation)
TOMS	Aerosols	whole atmosphere	Aerosol Index (AI)	1.0° X 1.25°	monthly means	
GSHAP	Peak ground acceleration (PGA) 10% chance of exceedance in 50 years	surface	m/s²	0.3° X 0.3°	time-invariant fields	
USGS	Global orography / topography (reduced to 0.3°)	surface	m	0.3° X 0.3°		
	Topographic tiles	surface	m; open sea = -500	30" X 30" (arcseconds)		

3. RESULTS USING FRIOWL

In this section, we present some results using the *FriOWL-v3.1* software and database. Due to space considerations, only three examples will be shown, namely analyses of cloud cover and integrated water vapour, followed by the presentation of a composite global map of three different overlaid layers. Please note that, while the images shown here are printed in greyscale (for publishing reasons), all FriOWL images can be displayed using a variety of colourful palettes, based on the IDRISI 32 software[10].

3.1 Analysis of clouds

Cloud cover is traditionally classified by meteorologists according to its height above the ground. Thus, high cloud cover (*hcc*) refers to cloud with a height of at least 6000 metres, mid-level cloud cover (*mcc*) refers to cloud between 2,000 and 6,000 metres, whilst low cloud cover (*lcc*) refers to cloud below 2,000 metres in elevation.

It is almost an astronomical convention to assume that the extremely large telescopes of the future will all be located on a mountain summit or plateau of greater than 2,000 metres in height, possibly even as high as 5,000 metres, in order to avoid any low cloud cover layers in the vicinity; indeed, if a site were not above low clouds, it would not be a candidate site. Therefore, we can limit our study to just *hcc* and *mcc*, by assuming *a priori* that any candidate site will lie above the *lcc* classification. Furthermore, we will limit our analyses here to cloud data only from the post-satellite period of 1989 to 2001. This is because there are considerable uncertainties in the estimation of cloud by the ERA40 re-analysis model, especially for periods during the early years of ERA40 project[11]. This is a problem common with all numerical weather models.

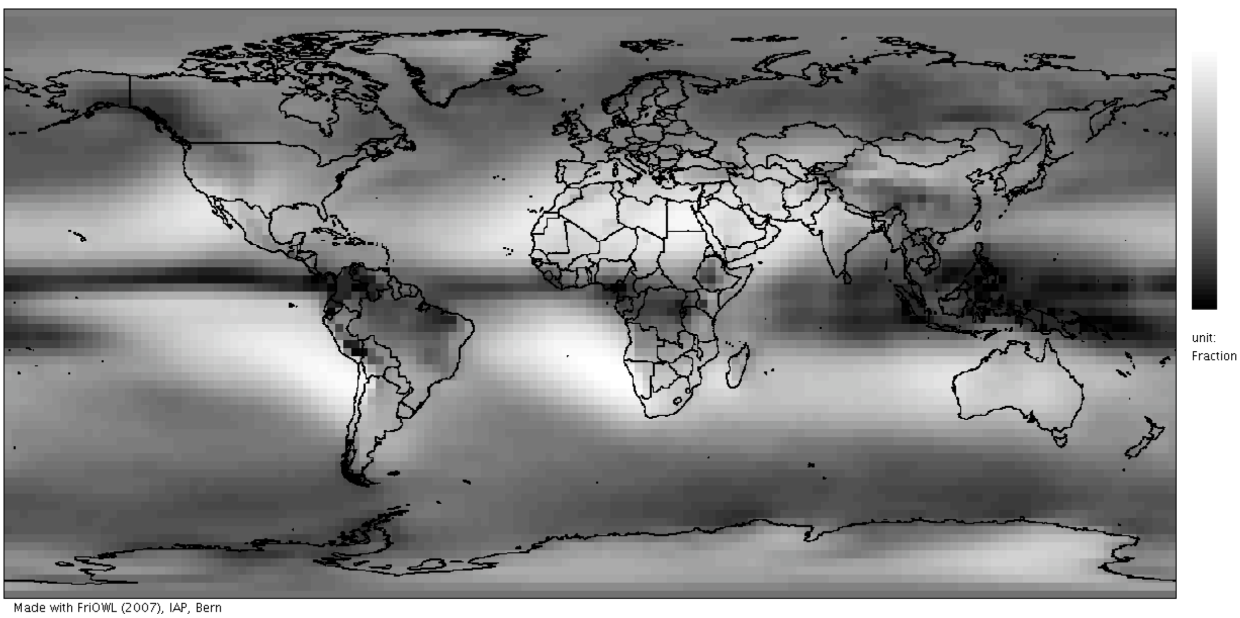

Figure 1: A *FriOWL-v3.1* map of the mean annual sum of ERA40 high and mid-level cloud cover (*hcc+mcc*), as calculated over the period 1989-2001. The values shown are the sum of the (decimalised) fraction of cloud cover of the high and mid-level categories; thus, the maximum possible is 2.00, the minimum possible value is 0.00 (although please note that the legend has been scaled to between 0 and 1. This map shows the approximate global distribution of cloudiness at a height of 2000 metres above the surface.

Figure 1 shows the mean annual (1989-2001) high and mid-level cloud cover for all regions on the earth, according to the ERA40 re-analysis model. The values shown are the sum of the (decimalised) fraction of *hcc* and *mcc* categories (*hcc+mcc*); thus the maximum possible value is 2.00, the minimum possible value is 0.00. The figure confirms the most cloud-free elevated regions of the earth and seem to justify the non-coincidental locations of the world's currently largest astronomical sites (except perhaps Hawaii). These observatories are essentially concentrated near four regional zones or 'tongues', namely (i) the south-east Pacific and northern Chile coastal zone (ii) Namibia and south-west Africa coast (iii) coastal California (USA and Mexico) and (iv) Canary Islands and western Morocco. Regular oscillations in the degree of cloudiness occur between the seasons (not shown), although the Namibian zone appears to be remarkably persistent all year round. In fact, it is a somewhat surprising result that the most cloud-free region above 2000 metres in the world lies near coastal Namibia and over the south-east Atlantic Ocean; detailed examination reveals that it is actually less cloudy than the Atacama desert of northern Chile. However, frequent low cloud and stratus plague these coastal regions near the sea surface; a high mountain summit is a pre-requisite to penetrate these stable surface layers.

Furthermore, it can be noted from Figure 1 that a fifth zone of very low *hcc+mcc*, centred near Egypt and stretching from the Sahara desert to almost Pakistan (referred to from now on as the "Arabic" zone) is evident, especially during the summer half of the year (not shown). There are many mountains above 2000 metres in this zone (2.629 metres at Mount St. Catherine, highest mountain in Egypt), but few astronomical observatories. Overall cloud statistics for this pixel compare favourably with those of Namibia and the northern Atacama. Indeed, this 'Arabic' zone is the only location on earth to report effectively zero cloud during the summer months. This area deserves further investigation by ESO and other research bodies. The deficiency in large telescopic facilities suitable for research across the Arabian peninsula has already been noted by [12].

Also interesting is the cloud-free area stretching from coastal Namibia (Brandberg, Gamsberg) to Saint Helena Island (15.9°S, 5.7°W). Brandberg is understood to be a site of local religious and cultural significance, however, so site surveys may not be permitted. Unfortunately, the island of St. Helena, which lies directly under the area of lowest *hcc+mcc* (mean value = 0.07) in Figure 1, reaches only to 818 metres at its highest point, and so is likely to be plagued by fog and low clouds; if it had higher mountains, it would be a prime candidate site.

3.2 Analysis of integrated water vapour (IWV)

As a second example, we will analyse integrated water vapour (IWV) using data from 700 hPa (*iwv700*) level. This particular level is chosen, because it corresponds to the approximate altitude of most candidate E-ELT sites (2,500 to 3,000 metres). Only data from the post-satellite period of the ERA40 re-analysis (1976-2001) are used here, due to inhomogeneity concerns in the global specific humidity dataset[13]. The units of IWV are kg/m^2, which is also equivalent to mm.

Figure 2 shows a reclassified *FriOWL-v3.1* map of ERA40 IWV at the 700 hPa level (*iwv700*), where pixels with *iwv700* values of greater than 4mm have been given a new boolean value of 0, and pixels less than 4mm have been reclassified with a new value of 1. This procedure has been accomplished using *FriOWL* in an attempt to highlight preferred regions. Of particular note in Figure 2 are the four reasonably symmetric 'tongues' of relatively low water vapour, stretching equatorwards and westwards, located on the eastern flanks of the zones of four main sub-tropical high pressure circulations (namely Aleutian high, Azores high, Easter Island high and south-east Atlantic high); the location of these 'tongues' has already been noted in the previous section on clouds (3.1). Of great prominence also are low values found in all polar regions; values are extremely low over Antarctica, which contribute to a very low infra-red background sky radiation there, by far the lowest on earth[14].

It is of no co-incidence that the aforementioned 'tongues' are located over regions of cool, upwelling equatorward-moving sea currents on the western sides of the main continents, and that many of the world's current largest astronomical observatories are located in areas near these 'tongues'. It is of interest, however, that the tongue on the eastern side of the Aleutian high, although crossing the mountains of California, does not stretch completely over either Hawaii (Mauna Kea observatory) or Baja California (San Pedro Martir observatory). Likewise, the tongue over the south-east Atlantic does not quite stretch over Namibia (Gamsberg, Brandberg). However, all of the Chilean sites lie within their respective 'tongue', as do the Canary Island observatories of La Palma and Tenerife (although not Morocco). Particularly interesting, however, and evident from Figure 2 is the separate, fifth tongue over Egypt, the Sinai Peninsula, Jordan and north-western Arabia (the 'Arabic' zone) where, as already stated, several mountain ranges reach over 2000 metres in height. Integrated water vapour values over the Sinai may approach those of the southern Atacama in Chile, at least at the 700 hPa elevation.

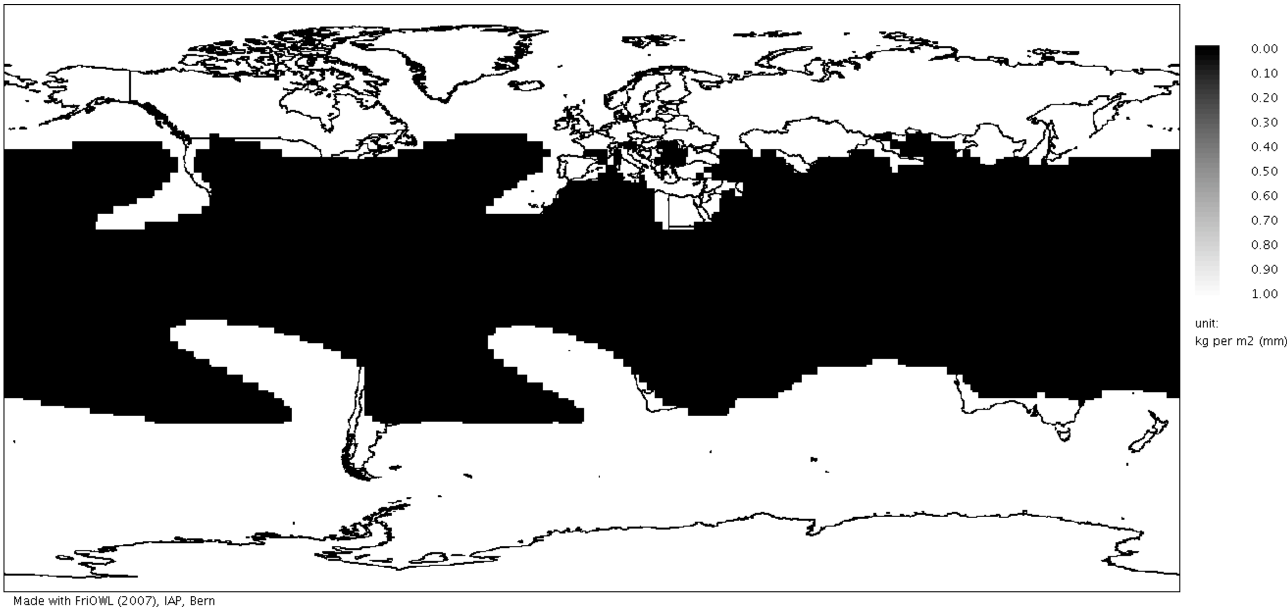

Figure 2: A reclassified *FriOWL-v3.1* map of mean annual (1976-2001) ERA40 integrated water vapour at 700 hPa (*iwv700*). All pixels with a *iwv700* of greater than 4 mm have been given a value of 0 (black); all pixel values less than 4mm are reclassified with a value of 1 (white). Note the predominance of five global tongues of low water vapour, stretching equatorwards and westwards on the eastern, descending arms of the main global high pressure Hadley cell circulations.

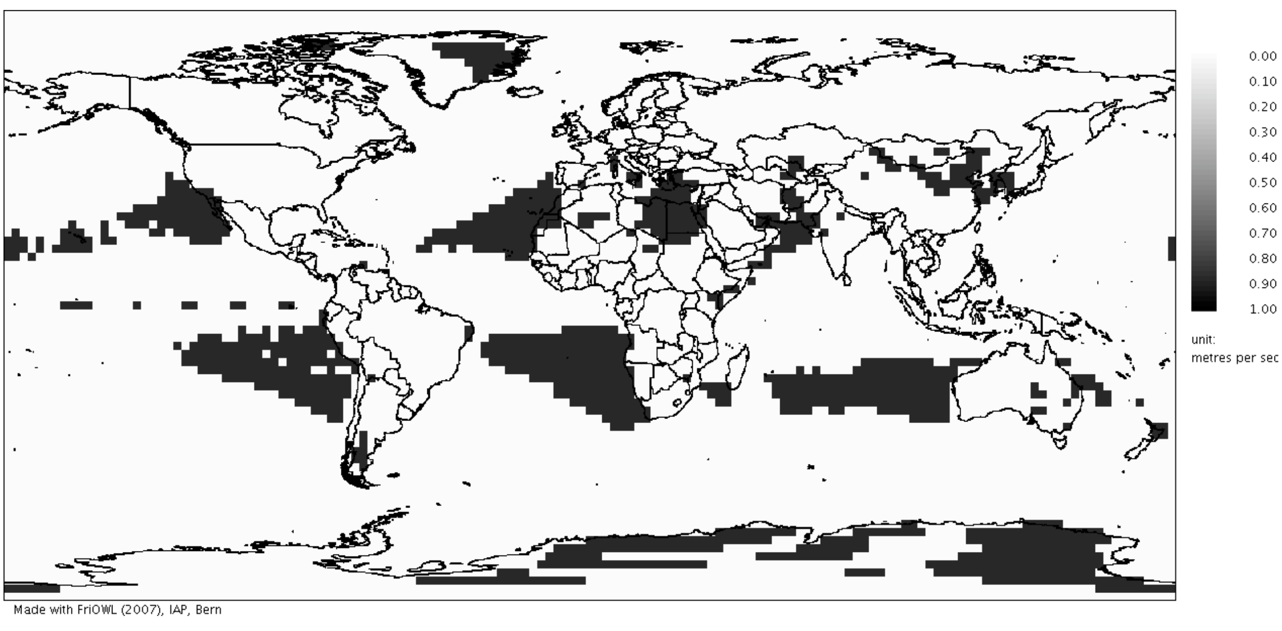

Figure 3: A reclassified *FriOWL-v3.1* map of mean annual (1991-2000) ERA40 mid-to-upper tropospheric vertical velocities (*w*), averaged over all vertical levels from 775 hPa to 200 hPa. All pixels with a *w* of greater than 2.5 cm/sec (gently descending air) have been given a value of 1 (black); all other pixels are reclassified with a value of 0 (white). Note the similarity of features in this image with Figure 2, identifying again the five global tongues' of gently descending stable airmasses.

Meanwhile, Figure 3 is a *FriOWL-v3.1* reclassified map of the mean annual (1991-2000) ERA40 mid-to-upper tropospheric vertical velocities (*w*), showing only areas of the globe where *w* exceeds a value of +2.5 cm/sec (a positive value means the air is sinking). The mid-to-upper troposphere in this instance is defined as the average of the values at the 775, 700, 600, 500, 400, 300, 250 and 200 hPa levels. Notice the remarkably similar patterns between Figures 2 and 3, although both maps are showing entirely different meteorological variables. As well as the usual five 'tongues' already identified, large areas of descending air can be seen to the west of Australia (but no mountains here) and near the edges of the Greenland and Antarctica ice caps – due to large scale katabatic wind drainage. Gently descending air usually means dry air, means stable air; that is why there is such good correlation between Figures 2 and 3.

3.3 Overlaying maps to make a *composite* map

One of the advantages of the *FriOWL-v3.1* software is the ability to to reclassify layers to show only regions of certain interest, and then to overlay these layers upon one another in order to make a single composite layer of new information. An example of this procedure is now shown in Figure 4, where we have created, using *FriOWL-v3.-1*, a new composite map based on three previously reclassified layers. This map was created by superimposing the following three layers:

(i) A reclassified cloud map, showing areas only where mean annual *hcc+mcc* <= 0.20
(ii) A reclassified integrated water vapour map, showing only areas where mean annual *iwv700* <= 4mm
(iii) A reclassified vertical velocity (*w*) map, showing only areas where 2.5 < mean annual *w* > 5.0 cm/sec

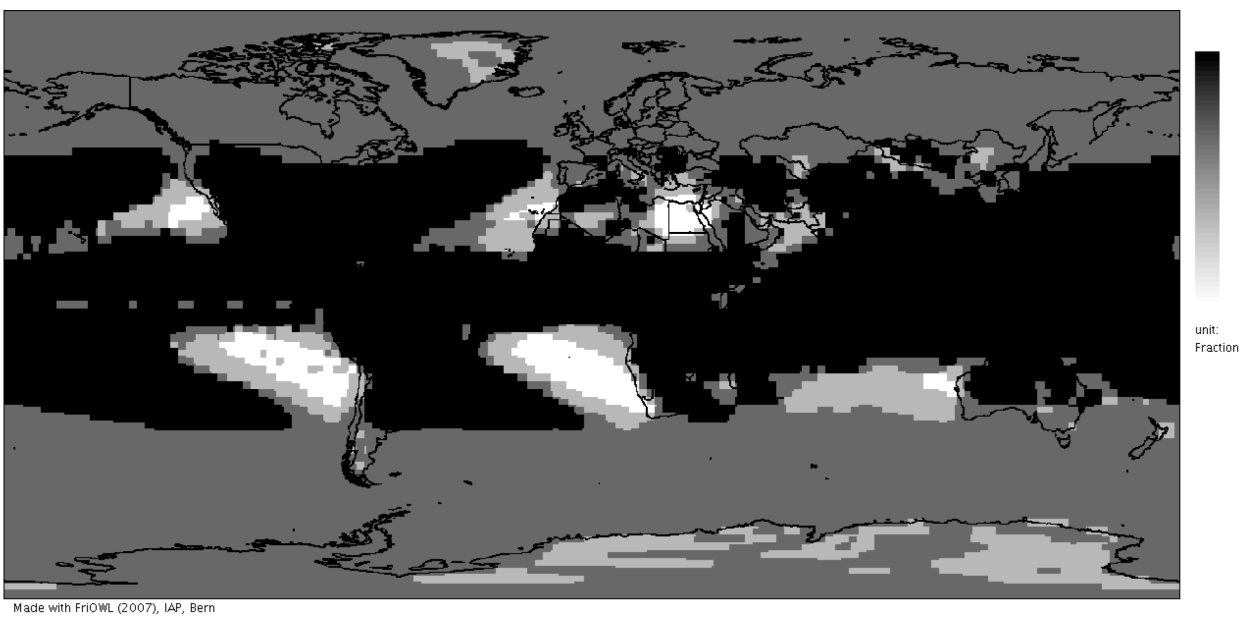

Figure 4: A composite *FriOWL-v3.1* map made of three different overlaid layers. The three layers are reclassified maps, composed of 0s and 1s, with the following criteria; (a) mean annual *hcc+mcc* cloudiness of less than 0.20 (if criteria is met, value = 1; if not, value =0); (b) mean annual *iwv700* of 4mm or less (if criteria is met, value = 1; if not, value =0); (c) mean annual mid-to-upper tropospheric velocities of between +2.5 and 5.0 cm /sec (if criteria is met, value = 1; if not, value =0). The composite map shown above is the sum of all of these reclassified layers. Thus, pixels with a value of 3 (white) in the above image show areas where all three of the aforementioned criteria are met; pixels with a value of 2 (light grey) show where 2 criteria are met; pixels with a value of 1 (dark grey) show where only 1 of the criteria are met; pixels with a value of 0 (black) show areas where none of the above criteria are met.

For each of the original three maps, in turn, all pixels which met the above criteria were given a boolean value of 1; all other areas were given boolean values of 0. Then, the three reclassified maps were overlaid upon one another, and their values summed, to make the final composite map as shown in Figure 4. As can be seen, there are only six regions on the earth where the above three criteria are fully met (white shade in Figure 4). They are as follows:

(1) Just offshore south-west USA and north-west Mexico
(2) Just offshore northern Chile, stretching north-westwards to Galapagos Islands
(3) Canary Islands (not Morocco)
(4) Large area off Namibian coast to Saint Helena Island
(5) Egypt and the Gulf of Aqaba / Eilat
(6) Just offshore western Australia

4. CASE STUDY OF ESO PARANAL

Mean annual seeing conditions at ESO Paranal (24.7°S, 70.4°W) have deteriorated significantly from approximately 0.65" in the early 1990s to nearly 1.0" during the period 1998-2006; the reason is thought to be related to a unforeseen climatic shift. Therefore, a special case study using *FriOWL-v3.1* output compared to the long-term ESO Paranal and La Silla mean monthly seeing and photometric statistics was conducted. In the first instance, monthly mean time series of a total of thirty-five different climatological parameters were extracted from *FriOWL* for the re-analysis gridpoints closest to Paranal (25.0°S, 70.0°W) and La Silla (30.0°S, 70.0°W). Each of these time series were then examined for correlation with the seeing and photometric statistics of each observatory over the period 1983 to 2006, in an attempt to validate *FriOWL* using the astronomical viewing data. Secondly, a variety of *FriOWL* maps were created to analyse the main atmospheric circulation patterns and anomalies over South America from 1983 to the present, with particular emphasis in determining any circulation changes that have occurred during the post-1998 period.

Detailed results of all the correlations will be presented in a separate paper, but they generally show that seeing at Paranal is strongly related to the surface windspeed and direction and near-surface circulation pattern. At La Silla, mid-tropospheric winds (700 to 500 hPa) seem to explain the seeing variations better, possibly due to its more southerly location being closer to frontal passages and the westerly wind belts. Photometric night fractions at both observatories are strongly correlated with the outgoing longwave radiation (OLR) and ERA40 total and high cloud cover datasets, although there are links with many of the other 35 climatological parameters also.

4.1 The Paranal Seeing Problem: use of FriOWL anomaly maps

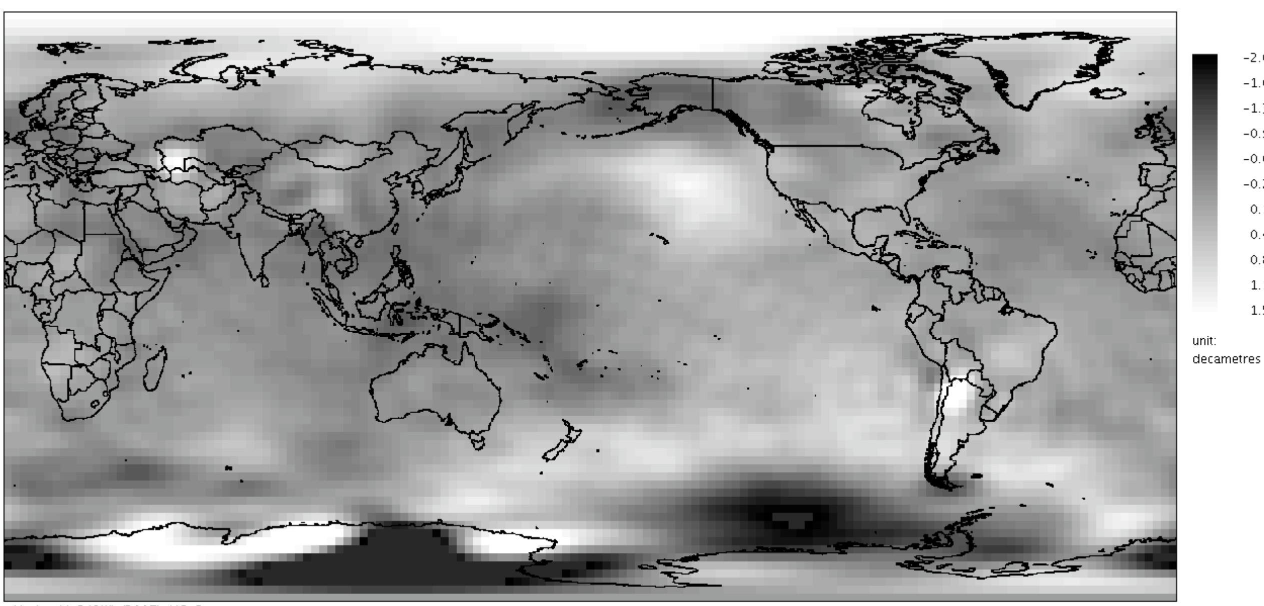

Figure 5: A *FriOWL-v3.1* map of the anomaly of 1000 hPa geopotential height of [October 1998 to September 2007] minus [October 1989 to September 1998]. Units are decametres (10 metres).

Meanwhile, Figure 5 shows the difference in global geopotential height at 1000 hPa level between October 1998 to September 2007 (poor seeing conditions at Paranal) and October 1989 and September 1998 (good seeing conditions). Although the 1000 hPa level is below the height of surface in northern Chile, the flow pattern at this level can still be considered as an approximation of the surface boundary layer conditions, because surface pressure and temperature values are extrapolated downwards when calculating the 1000 hPa geopotential height. The given units of geopotential height are decametres (dam, or 10 metres). Positive anomalies in this map means that the geopotential height has been higher during the latter nine-year period (October 1998 to September 2007; poor seeing conditions) than during the former period (October 1989 to September 1998; good seeing conditions).

A number of very interesting features are apparent from Figure 5. Firstly, a very strong positive anomaly (anticyclonic) of geopotential height can be seen over north-western Argentina / northern Chile, just to the east / south-east of Paranal during the latter nine-year period (poor seeing conditions). Outside of Antarctica (where the anomalies may not be realistic), this is one of the strongest anomalies in the whole world during this period. This particular anomaly seems to occur within a much wider arc of slightly weaker, positive anomalies stretching across the whole of South Pacific Ocean, with a marked negative (cyclonic) anomaly off the Antarctic coast at 100-120°W. Other similar anomalous patterns occur over the North Pacific Ocean. This features may be manifestations of what is known as the Interdecadal Pacific Oscillation (IPO[15]).

4.2 The Interdecadal Pacific Oscillation (IPO)

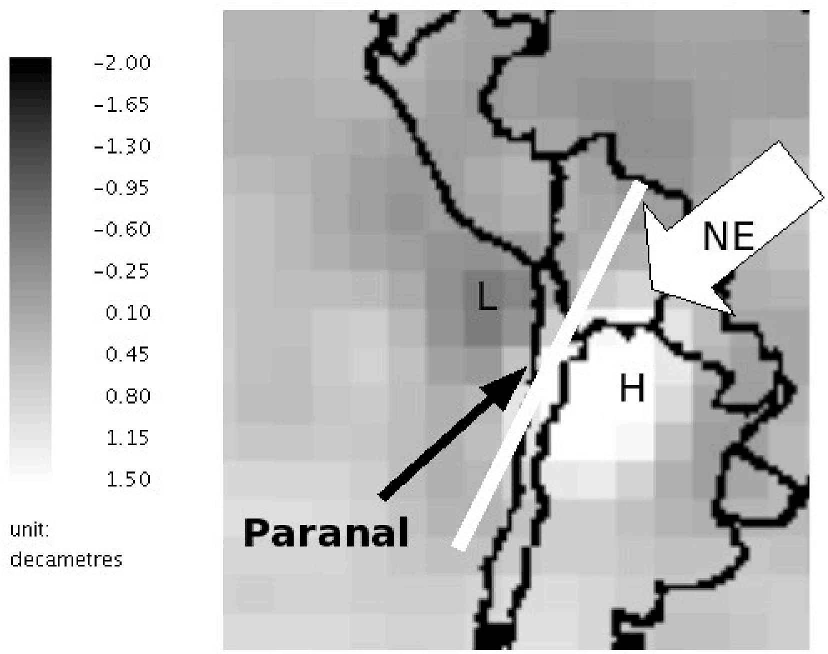

Figure 6: A zoom-into Figure 5, with depictions of the anomalous low ('L') and high ('H') geopotential height centres during 1998-2007 (poor seeing conditions at Paranal), to the north-west and south-east of Paranal observatory, respectively. The axis between the two anomalies is marked by the thick white line. Given geostropic balance between the pressure forces, and a slight veering of the wind due to surface frictional forces, the resulting anomalous wind direction at Paranal is north-easterly, as indicated by the thick white arrow ('NE').

The Interdecadal Pacific Oscillation (IPO) is an El-Nino-Southern-Oscillation (ENSO) style phenomenon that affects sea surface temperatures and consequently air circulation patterns. Unlike ENSO, however, which operates on timescales of 6-18 months (with a typical return period of 5 to 7 years) the IPO has a period of oscillation once every 20-30 years.

Also, whilst ENSO is largely restricted to equatorial and sub-tropical Pacific regions, the IPO is manifest over the whole of the North and South Pacific Oceans. It is said to be a larger form of a similar oscillation known as the Pacific Decadal Oscillation (PDO), which operates in the North Pacific region[16]. Recently, during 1998, the IPO switched to a negative phase, after being in a positive phase since the mid-1970s.

Further analyses and graphs (not shown) confirm that a shift southwards has occured in the axis of highest geopotential height in the vicinity of Paranal (70°W) during the post-1998 period. During the earlier 1989 to 1998 period, the area of highest geopotential height generally occurred near 21°S, allowing a prevailing west or northwesterly flow over Paranal. However, from 1998 to 2007, the axis of highest geopotential height shifted south to between 25 and 27°S. The shift is most apparent at near-surface heights (1000, 925 and 850 hPa levels) but is absent at higher levels (700, 500 hPa). Given geostropic balance of pressure gradients, the consequence of this shift is to allow more frequent north-easterly (cyclonic) winds to blow north of 27-25°S. Indeed, it has been shown by Sarazin[†] that poorer seeing conditions at Paranal observatory are due to an increase in the frequency of night-time north-easterly boundary layer winds that blow across a long fetch of mountaineous terrain. This is in contrast to the previously predominant north-westerly wind which blew with a fetch across the Pacific Ocean, giving less opportunities for mountain turbulence and better seeing conditions. These findings are summarised in Figure 6, which is zoom-into Figure 5, overlaid by schematic depictions of cyclonic anomaly centres and anomalous wind arrows for the latter 1998 to 2007 period.

Further work will involve investigating the degree of correlation between the IPO and a selection of geopotential height indices, such as the gradient between the anomalous cyclonic and anticyclonic centres shown in Figure 6, or the strength of the Antarctica cyclonic anomaly shown in Figure 5.

5. CONCLUSIONS

The FriOWL software has demonstrated its use in site selection studies in terms of (i) being a single portal for a large database of long-term global climatic and geophysical data information, and in (ii) providing the means to investigate, study, analyse and manipulate the data.

Egypt and the Sinai Peninsula, including the whole area surrounding the Gulf of Aqaba (Eilat) has been identified as possible candidate region for large telescope projects, an area which remains largely unexploited to date. Several mountain peaks reach above 2,000 metres elevation in this region. Summertime cloudiness in this area is the lowest of anywhere in the world and integrated water vapour values at 700 hPa may approach those of the southern Atacama in Chile at the same elevation.

In Namibia, the coastal peak of Brandberg (2,600 metres evelation) has also been identified as a site worthy of considerable interest, but it is understood that the mountaintop is a site of local religious and cultural significance, which would preclude any on-site construction or astronomical site surveys.

A case study examination of ESO Paranal using FriOWL maps reveals that significant deterioration in seeing conditions at Paranal since 1998 appears to be related to very strong increase in 1000 hPa geopotential height to south-east of observatory, when compared to previous years. A shift south of the axis of the main high pressure zone from 21°S to 25-27°S has occurred, and this appears to be responsible for an increasing frequency of north-easterly winds giving a greater fetch of wind over land. There is a possible link with the Interdecadal Pacific Oscillation. The optimum location for an observatory in Chile may now be nearer 27-30°S, rather than 21-25°S.

The lesson to be learned from Paranal is that there is a need for applications like *FriOWL*, because if one does not look at long-term climatic datasets, you may miss something. It is also extremely important to consider possible changes of climate and circulation patterns in the future due to global warming, which should not be underestimated.

† *http://www.eso.org/gen-fac/pubs/astclim/paranal/asm/verif/longverif.html*

6. A NEW NAME FOR FRIOWL: S-ELT

It will be apparent to those readers *au fait* with site selection issues, that at the time of writing (June 2008), the *FriOWL* acronym and software name has already served its purpose (following the demise of *OWL* and change of *FriOWL* headquarters from Fribourg to Bern, Switzerland). Therefore, with the dawn of the new E-ELT era already well upon us, the introduction of a new name is appropriate. The proposed new name is ***S-ELT.*** which can be understood as an acronym of any the following three phrases, or their combinations:

(i) Site sELection Tool
(ii) Site search for the E-eLT
(iii) Swiss ELT project

Finally, it may also have not escaped the attention that this name is also a phonological pun on another well-known telescope project, when pronounced with a CELTic accent!

ACKNOWLEGDEMENTS

The ECMWF ERA-15 and ERA-40 reanalysis data used in this study have been provided by ECMWF, Shinfield Park, Reading, England and have been obtained from the ECMWF data server at http://data.ecmwf.int/data/. The NOAA OLR and NCEP-NCAR reanalysis data have been provided by the NOAA-CIRES Climate Diagnostics Center and NOAA/OAR/ESRL PSD, Boulder, Colorado, USA, available at http://www.cdc.noaa.gov. The CCCma CGCM1 data used in this work have been provided by the Canadian Centre for Climate Modelling and Analysis, Environment Canada, Victoria, British Columbia, Canada, available at http://www.cccma.bc.ec.gc.ca. The TOMS Aerosol Index data has been provided by the Chemistry and Dynamics Branch of the NASA Goddard Space Flight Center in Greenbelt, Maryland, USA, available at ftp://toms.gsfc.nasa.gov/ and http://toms.gsfc.nasa.gov/. The global seismic data set is provided by the Global Seismic Assessment Hazard Program, available at http://www.seismo.ethz.ch/GSHAP/. The USGS digital elevation model data was provided by the Earth Resources Observation and Science (EROS) group of the United States Geological Survey (USGS), Sioux Falls, South Dakota, USA, available at http://edc.usgs.gov/products/elevation/gtopo30/gtopo30.html. Java is a registered trademark of Sun Microsystems Incorporated. This work has been completed between 2002 and 2008 at the Universities of Fribourg, Bern and Zürich (Switzerland) under contract with the European Southern Observatory, Garching, Germany. The authors express thanks and gratitude to all of persons who have been involved in this project or who have helped in any way.

REFERENCES

[1] Graham, E., [A site selection tool for large telescopes using climate data], Inauguraldissertation der Philosophisch-naturwissenschaftlichen Fakultät (PhD thesis), University of Bern (2008).

[2] Graham, E., Sarazin, M.S., Beniston, M., Collet, C., Hayoz, M., Neun, M. and Goyette, S. "Site selection for OWL using past, present, and future climate information". Proceedings of The International Society for Optical Engineering (SPIE), 5489, 102-112 (2004).

[3] Graham, E., Sarazin, M., Beniston, M., Collet, C., Hayoz, M., Neun, M. and Casals P. "Climate-based site selection for a Very Large Telescope using GIS techniques". Meteorological Applications, 12, 77-81 (2005).

[4] Sarazin, M. Graham, E. and Kurlandczyk, H. "FriOWL – a site selection tool for the European Extremely Large Telescope (E-ELT) Project". The Messenger, 125, 44-47 (2006).

[5] Kalnay, E., Kanamitsu, M., Kistler, R., Collins, W., Deaven, D., Gandin, L., Iredell, M., Saha, S., White, G., Woollen, J., Zhu, Y., Chelliah, M., Ebisuzaki, W., Higgins, W., Janowiak, J., Mo, K.C., Ropelewski, C., Wang, J., Leetmaa, A., Reynolds, R., Jenne, R. and Joseph, D. "The NCEP/NCAR Reanalysis Project". Bulletin American Meteorological Society, 77, 437-471, (1996).

[6] Uppala, S.M., Kållberg, P.W., Simmons, A.J., Andrae, U., da Costa Bechtold, V., Fiorino, M., Gibson, J.K., Haseler, J., Hernandez, A., Kelly, G.A., Li, X., Onogi, K., Saarinen, S., Sokka, N., Allan, R.P., Andersson, E., Arpe, K.,

Balmaseda, M.A., Beljaars, A.C.M., van de Berg, L., Bidlot, J., Bormann, N., Caires, S., Chevallier, F., Dethof, A., Dragosavac, M., Fisher, M., Fuentes, M., Hagemann, S., Hólm, E., Hoskins, B.J., Isaksen, L., Janssen, P.A.E.M., Jenne, R., McNally, A.P., Mahfouf, J.-F., Morcrette, J.-J., Rayner, N.A., Saunders, R.W., Simon, P., Sterl, A., Trenberth, K.E., Untch, A., Vasiljevic, D., Viterbo, P. and Woollen, J. "The ERA-40 re-analysis". Quarterly Journal of the Royal Meteorological Society, 131, 2961-3012 (2005)

[7] Giardini, D., Grünthal, G., Shedlock, K.M. and Zhang, P. "The GSHAP Global Seismic Hazard Map". Annali di Geofisica, 42 (6), 1225-1230, (1999).

[8] USGS. "GTOPO30: The 30 arcsecond digital elevation model (DEM) from the United States Geological Survey (USGS)". Center for Earth Resources Observation and Science (EROS), Sioux Falls, SD, USA, (1996). Available online at: http://edc.usgs.gov/products/elevation/gtopo30/gtopo30.html

[9] Flato, G.M., Boer, G.J., Lee, W.G., McFarlane, N.A., Ramsden, D., Reader, M.C. and Weaver, A.J. "The Canadian Centre for Climate Modelling and Analysis Global Coupled Model and its Climate". Climate Dynamics, 16, 451-467 (2000).

[10] Eastman, R. IDRISI 32, Vers. I32.22, Clark Laboratories, Clark University, Worcester, MA, USA, (1987-2002).

[11] Chevallier, F., Kelly, G., Simmons, A.J., Uppala, S. and Hernandez, A. "High clouds over oceans in the ECMWF 15-year and 45-year re-analyses". ERA-40 Project Report Series No.11. ECMWF, Shinfield Park, Reading, England (2003). Available online at: http://www.ecmwf.int/publications/library/do/references/list/192

[12] Sultan, A.H. and Graham, E. "Search for an astronomical site on the Arabian peninsula". Abstract for UN/ESA/NASA workshop on International Heliophysical Year, Abu-Dhabi and Al-Ain, United Arab Emirates, 20-23 November 2005 (2005).

[13] Bengtsson, L., Hagemann, S. and Hodges, K.L. "Can climate trends be calculated from reanalysis data ?" Journal of Geophysical Research, 109, D11111, (2004).

[14] Chamberlain, M.A.; Ashley, M.C.B.; Burton, M.G.; Phillips, A.; Storey, J.W.V. and Harper, D.A. "Mid-Infrared Observing Conditions at the South Pole". The Astrophysical Journal, 535(1), 501-511, (2000).

[15] Folland, C. K., Renwick, J. A., Salinger, M. J. and Mullan, A. B. Relative influences of the Interdecadal Pacific Oscillation and ENSO in the South Pacific Convergence Zone. Geophysical Research Letters, 29 (13), 21-1-21-4, (2002).

[16] Mantua N. J., Hare S.R., Zhang Y., Wallace J.M. and Francis R.C."A Pacific interdecadal climate oscillation with impacts on salmon production". Bulletin of the American Meteorological Society, 78, 1069–1079, (1997).